Journal of International Scientific Publication:
Materials, Methods & Technologies, Volume 4, Part 1

NUMERICAL SIMULATION OF PLASMA FLOW DYNAMICS IN A MAGNETIC CHANNEL

Konstantin V. Vshivkov[1]

[1]Institute of Laser Physics, Siberian Branch of the Russian Academy of Sciences,

Ac. Lavrentiev ave., 13/3, Novosibirsk 630090, Russia

Abstract

The problem of interaction of a plasma flow with an inhomogeneous magnetic field is considered. The field is generated by a magnetic coil system. Field lines along the coil axis form a channel which is used to control a plasma flow. A 3D hybrid code has been used. Regimes during plasma flow separation from the field lines at channel outlet have been investigated. The work results can be used for a study of processes taking place in a magnetic nozzle.

Key words: *3D hybrid code, particle-in-cell (PIC) method, system of Vlasov- Maxwell's equations, numerical calculations*, *propulsion plasma devices, magnetic nozzle, inhomogeneous magnetic field.*

1. INTRODUCTION

A magnetic nozzle is an important component of propulsion plasma devices using a strong guiding magnetic field to control a plasma flow. It is a channel with a magnetic force tube of varying section connected to the plasma source. The nozzle has to accelerate the incoming plasma flow by a transformation of its inner energy into kinetic energy of directed motion. First, the tube section at the accelerating region along the channel is decreased, and then is expanded as the Laval nozzle. At the region of the tube widening the ejecting plasma has to become free from the field lines to create a propulsion. If the plasma stays frozen into magnetic field lines then there is no resulting propulsion can take place.

A separation of the plasma stream from the engine magnetic field is the key problem for numerous plasma engine devices with a magnetic nozzle. Therefore, a research in this area is the important part of works dealing with a big class of plasma engine technologies in the space and requires hard work.

There are two possibilities for solving the problem of plasma stream separation. The first one consists in the violation of the limiting frozen-in condition by a recombination or some other mechanism (Gerwin et al., 1990). The second possibility uses the frozen-in condition and assumes that the plasma stretches the magnetic field lines along the flow and is separated from the engine along with a portion of magnetic field. This scenario of magnetic field breaking resembles one which takes place in the solar wind during moving away from the Sun (Parker, 1958).

There is a difference between plasma separation and separation of isolated charged particles. A single ion tears off a magnetic field line easily if its gyroradius is more than a field characteristic scale (it is said that the ion is "not magnetized"). However, in the case of a sufficiently dense plasma, ions can escape only with electrons to maintain a quasineutrality of plasma. The electrons, the gyroradius of which are very small, are attached closely to the magnetic field lines, and, the plasma can remain attached to the field lines even when the ions are not magnetized. Because of this restriction it is very hard to achieve a separation by a drift motion of particles across the magnetic field lines (Hooper, 1993).

The ion and electron recombination in plasma at which neutral particles are generated is not a preferable separation mechanism as recombination velocities in the area of the nozzle widening are very small generally. The effects of finite resistivity could lead to the plasma separation by means of a plasma diffusion across the magnetic field and a reconnection of magnetic field lines. A lengthwise impulse obtained by plasma within the nozzle can allow the plasma to intersect resistively the diverging magnetic field lines at the nozzle outlet. However, a resistive plasma separation does not solve completely the separation problem as a propulsion is essentially reduced due to resistive losses in the plasma friction in the nozzle magnetic field regardless of quantity of the Reynolds magnetic number (Gerwin, 1990).

This understanding leads us to the need to investigate different configurations of the magnetic nozzle and determine the conditions of the "frozen-in separation" of plasma from the nozzle magnetic field.

A plasma flow outside the nozzle consists of two parts: an unperturbed main flow with straight magnetic field lines and a depression wave at the edge of the main flow. It had been shown in (Arefiev and Breizman, 2005) that an ejecting flow is detached from the nozzle along with a residual magnetic field while the flow is superalfvenic. At the separation process the plasma expands and the flow partially loses its direction and becomes less collimated than the flow inside the nozzle. This radial expansion caused by the balance violation between the magnetic field pressure and plasma pressure in the stream.

Two main factors influencing a nozzle efficiency are the geometric convergence of the nozzle magnetic field lines and additional radial propagation of the flow coming out on its edges. The relation of these factors which limits a geometry of the magnetic nozzle had been established in (Arefiev and Breizman, 2005). The theoretical estimations show that the efficiency factor of a plasma engine can achieve 80%. On the current stage it is necessary to make numerical calculations to determine the efficiency factor of the nozzle for the considered magnetic field geometry used for the specific type of the plasma engine.

The basic equations for the numerical model introduced in this article are the Vlasov's equation for ions and the fluid moment equations for electrons. At present time the most effective and universal method for solving the Vlasov's equation is the particle-in-cell (PIC) method.

2. STATEMENT OF THE PROBLEM

The three-dimensional problem of interaction of a plasma flow with an inhomogeneous magnetic field is considered. A geometry of the considered problem is illustrated in Fig. 1. Here the Cartesian coordinates (*X,Y,Z*) are introduced. The field is generated by a system of infinitely thin magnetic coils with the radius R_c and the current I_c. The current coil centers are located on the X-axis at some distance *D* from each other. The magnetic force lines along the coil axis form a channel which is used to control a plasma flow.

At initial time the plasma at the channel entrance has a parallelepiped shape. The plasma is characterized by linear scales (Z_p, X_p, Y_p), a location along the X-axis, an initial velocity V_0 along X-axis and, also, a big number *N* of model particles. The initial distributions of the particle positions and velocities are assumed to be uniform. The initial magnetic field is calculated by using the Bio-Savar-Laplace law. At next time stages the plasma enters into magnetic channel. It accelerates there under the influence of the magnetic field.

In the present study the plasma dynamics at the magnetic channel outlet has been investigated. Also, the regimes at which a plasma separation from magnetic force lines takes place has been studied.

In this study we use the 3D hybrid PIC code (Nagamine and Nakashima, 1999, Vchivkov, Nakashima et al., 2003) based on the numerical model given by (Hockney, 1981, Harned, 1982, Horowitz, 1989). The hybrid code treats ions as individual particles and electrons as a fluid. This approach is valid when the system behavior is dominated by ion physics.

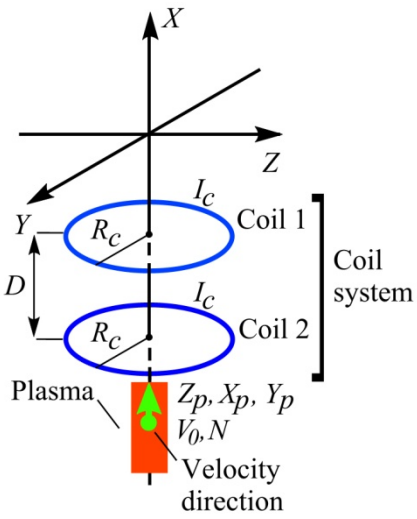


Fig. 1. Geometry of the problem.

Our model of collisionless plasma consists of the kinetic Vlasov's equation for an ion component:

$$\frac{\partial f_i}{\partial t} + \vec{v}\frac{\partial f_i}{\partial \vec{r}} + \vec{F_i}\frac{1}{m}\frac{\partial f_i}{\partial \vec{v}} = 0, \qquad (1)$$

$$\vec{F_i} = q_i\left(\vec{E} + \vec{v} \times \vec{B}\right),$$

a momentum equation for an electron fluid:

$$n_e m_e \left(\frac{d\vec{v}_e}{dt}\right) = -en_e\left(\vec{E} + \vec{v}_e \times \vec{B}\right) - \nabla P_e, \qquad (2)$$

and the Maxwell's equations (for plasma region):

$$\nabla \times \vec{B} = \mu_0 \vec{j} + \frac{1}{c^2}\frac{d\vec{E}}{dt}, \qquad (3)$$

$$\nabla \times \vec{E} = -\frac{\partial \vec{B}}{\partial t}. \quad (3)$$

To determine the electric field in vacuum we use the following equation:

$$\nabla \cdot \vec{E} = 0, \quad (4)$$

it leads to the Laplace equation for the electric potential

$$\Delta\varphi = 0.$$

The current density involved in the Maxwell equations is calculated from the distribution functions of the ions by using the following formula:

$$\vec{J} = \sum_i q_i \int f_i \vec{v} d\vec{v}.$$

Here, the index i indicates ions, f_i is the distribution function of the ions, $f_i \equiv f_i(\vec{r}, \vec{v}, t)$ ($\vec{r}$, $\vec{v}$ and t are the vector of particle positions, vector of particle velocities and time, respectively), q_i is the particle charge, m is the particle mass, $\vec{J}$ is the current density, and μ_0 is the vacuum magnetic permeability. $\vec{E}$ and $\vec{B}$ are the intensities of electric and magnetic fields, respectively, m_e is the electron mass, n_e is the electron density, e is the elementary electric charge, P_e is the electron pressure given by

$$P_e = n_e T_e,$$

where T_e is the electron temperature and it is assumed to be zero for simplicity.

The boundary conditions taken here for the field quantities are that the spatial differences of the normal components are set to be zero at the surface of the calculation region. When the plasma ions reach the calculation region boundary, the ion velocity is set to be zero.

The electrons are approximated as a massless fluid, so the left-hand side of (2) becomes zero. Also, it is taken into account that $T_e = 0$ and we obtain

$$\vec{E} = -\vec{v}_e \times \vec{B}. \quad (5)$$

The Ampere's law (3) with the Darwin approximation, which indicates that high-frequency electromagnetic waves do not exist, reduces to

$$\nabla \times \vec{B}_p = \mu_0(\vec{J}_e + \vec{J}_i), \tag{6}$$

where $\vec{B}_p$ is the magnetic field generated by the plasma current density and it is derived from the equation $\vec{B}_p = \vec{B} - \vec{B}_{ext}$, where $\vec{B}_{ext}$ is the external magnetic field. Substituting $-en_e\vec{v}_e$ for J_e in the Ampere's law (6) , solving for $\vec{v}_e$, and substituting the $\vec{v}_e$ into (5), we obtain

$$\vec{E} = \frac{1}{\mu_0 Z e n_i}(\nabla \times \vec{B}_p) \times \vec{B} - \frac{1}{Z e n_i}\vec{J}_i \times \vec{B}. \tag{7}$$

We assume a quasineutrality and set the ion charge density equal to the electron charge density, i.e.

$$Zn_i = n_e$$

in equation (7), where Z is the ion charge number. Equation (7) includes the terms inversely proportional to the ion density n_i. In the vacuum region, these terms must cause a numerical infinity. We solve the Laplace equation to obtain the electric field in the vacuum region.

3. METHOD OF SOLVING VLASOV'S EQUATIONS

From the mathematical standpoint the Vlasov's equation is the equation of hyperbolic type, which can be written in Euler or Lagrangian coordinates (Tajima, 1989, Vshivkov et al., 2001). These two terms were adopted from hydrodynamics (Kochin et al., 1963).

In Euler coordinates the plasma characteristics are functions that are defined in a coordinate system which is fixed on space. When the Euler coordinates are applied, the usage of finite - difference schemes is appropriate for the problem. In the schemes the values of grid functions that are defined at nearby nodes of introduced grid system are connected with each other by the approximation of derivatives.

The approach that is related to the name of Lagrange is as follows: the plasma is considered as a set of particles. Then any evolution characteristics of the plasma are defined as trajectories of the particles. In 6 - dimensional space, when the Lagrangian coordinates are used, it is also possible to introduce a spatial grid system at the nodes of which values of the functions are given. Thus, the coordinates of nodes are connected with plasma moving, that usually is a serious disadvantage, when the equations are solved by finite - difference methods, because in the course of solution there occurs a deformation of the Lagrangian grid. And this renders the approximation of spatial derivatives impossible.

The Vlasov's equation in Lagrangian coordinates becomes as follows:

$$\frac{df}{dt} = 0,$$

i.e, there are no space and velocities derivatives in the equation. Its solution indicates that the value of the distribution function is not changed in motion along the characteristic curve of equation and does not depend on the values of the distribution functions in other points of space.

The characteristic equations are as follows:

$$\frac{d\vec{v}_i}{dt} = \frac{Ze}{m_i}\left(\vec{E} + \vec{v}_i \times \vec{B}\right),$$
$$\frac{d\vec{r}_i}{dt} = \vec{v}_i. \tag{8}$$

From the equations the particle velocity $\vec{v}_i$ and the coordinate $\vec{r}_i$ are defined. In PIC method the characteristic equations define the paths of the plasma particles.

On the base of the description of Vlasov's equation in Lagrangian variable the PIC method is developed. The amount of chosen particles is determined by the necessary accuracy of solution and available computer resources (memory and speed). It follows that the PIC method reduces the problem of solving the Vlasov's equation in a 6 - dimensional space to the problem of integrating the equations of motion for individual particles.

In this study, for the equations (8) we use the scheme as follows:

$$\frac{\vec{v}_i^{n+1/2} - \vec{v}_i^{n-1/2}}{\Delta t} = \frac{Ze}{m_i}\left\{\vec{E}^n + \frac{1}{2}\left(\vec{v}_i^{n+1/2} + \vec{v}_i^{n-1/2}\right) \times \vec{B}^n\right\}, \tag{9}$$

$$\frac{\vec{r}_i^{n+1} - \vec{r}_i^{n}}{\Delta t} = \vec{v}_i^{n+1/2}. \tag{10}$$

Here Δt is the time step, index n indicates the moment of time, in which the desired function is calculated. The coordinates of the particles are calculated at $t^n = n\Delta t$ and velocities are calculated at $t^{n+1/2} = (n + 1/2)\Delta t$. The scheme is called as leapfrog scheme. It is a time-centered difference scheme, therefore it is second order accurate in time.

Model particles are moving along the same trajectories and with the same velocities as the real ions and electrons. Number of the model particles in the small volume, as in the real plasma, determines the density of these particles. Therefore the properties of real and model plasmas are similar. However, some features of the model plasma change greatly from the real plasma. For instance, the length of the free path in the model plasma is much less, but the frequency of collisions is much greater than in the

real plasma (Tajima, 1989, Hockney, 1981). Model plasma has a very high level of heat noise. For the elimination of these defects particles of finite size are used in the method.

PIC method has another important technological property such that the particles moving in each cell depend only on the values of electrical and magnetic fields in this cell and do not depend on coordinates and velocities of other particles. Therefore such cells together with the particles in them can be considered independently. The fact allows to easily modify a code, which realizes the PIC method, for solving another problems.

Only geometrical model, initial and boundary conditions and solving Maxwell equations must be changed. Particles motion inside the cells obeys common laws, independent of problems (Vshivkov, 2001).

Independence of particles motion permits parallel algorithms for solving the particles motion equation and calculations of density of plasma and average velocities of particles. Parallel algorithms give an opportunity to use modern multiprocessor computers for essential reduction of the time of solving the tasks. This, in turn, makes it possible to enlarge the amount of model particles and thus raise accuracy of calculations, hence more fine research of physical processes can be achieved (Vshivkov, 2001).

4. METHOD OF SOLVING MAXWELL'S EQUATIONS

The time advance of field quantities given by equations (3) and (7) is accomplished by a predictor - corrector algorithm (Harned, 1982, Horowitz et all., 1989). If the quantities $\vec{J}_i^{n+1/2}$, $\vec{v}_i^{n+1/2}$, $n_i^{n+1/2}$, $\vec{B}^n$ and $\vec{E}^n$ are known, the magnetic field is advanced by

$$\vec{B}^{n+1/2} = \vec{B}^n - \frac{\Delta t}{2}\nabla \times \vec{E}^n \tag{11}$$

and the electric field is calculated as follows:

$$\vec{E}^{n+1/2} = \frac{1}{n_i}\left\{\frac{1}{\mu_0 Ze}\left(\nabla \times \vec{B}_p^{n+1/2}\right) \times \vec{B}^{n+1/2} - \frac{1}{Ze}\vec{J}_i^{n+1/2} \times \right.$$
$$\left. \times \vec{B}^{n+1/2} - \frac{T_e}{e}\nabla n_i^{n+1/2}\right\}. \tag{12}$$

A prediction is then made for $\vec{E}^{n+1}$ and $\vec{B}^{n+1}$ by

$$\vec{E}_{pred}^{n+1} = -\vec{E}^n + 2\vec{E}^{n+1/2}, \tag{13}$$

$$\vec{B}_{pred}^{n+1} = \vec{B}^{n+1/2} - \frac{\Delta t}{2}\nabla \times \vec{E}_{pred}^{n+1}. \tag{14}$$

Using the predicted fields, a predictor particle move is performed to obtain $n_{i,pred}^{n+3/2}$ and $J_{i,pred}^{n+3/2}$ after which $\vec{B}_{pred}^{n+3/2}$ and $\vec{E}_{pred}^{n+3/2}$ are predicted by

$$\vec{B}_{pred}^{n+3/2} = \vec{B}_{pred}^{n+1} - \frac{\Delta t}{2} \nabla \times \vec{E}_{pred}^{n+1}, \tag{15}$$

$$\vec{E}_{pred}^{n+3/2} = \frac{1}{n_i}\left\{\frac{1}{\mu_0 Ze}\left(\nabla \times \vec{B}_p^{n+3/2}\right) \times \vec{B}_{pred}^{n+3/2} - \frac{1}{Ze}\vec{J}_{i,pred}^{n+3/2} \times \right.$$
$$\left. \times \vec{B}_{pred}^{n+3/2} - \frac{T_e}{e}\nabla n_{i,pred}^{n+3/2}\right\}. \tag{16}$$

Finally, the new electric and magnetic fields are obtained from

$$\vec{E}^{n+1} = \frac{1}{2}\vec{E}^{n+1/2} + \frac{1}{2}\vec{E}_{pred}^{n+3/2}, \tag{17}$$

$$\vec{B}^{n+1} = \vec{B}^{n+1/2} - \frac{\Delta t}{2}\nabla \times \vec{E}^{n+1}. \tag{18}$$

The particle position can now be advanced to $n+3/2$ using these new field quantities. The electric and magnetic fields are stored on different grids.

The predictor - corrector algorithm is of the second order accuracy in time and space. The time step is limited by a Courant - Friedrichs - Lewy (CFL) condition $\Delta t < h/V_0$, where h is the mesh size and V_0 the initial velocity of the particles. An additional constraint on the time step for numerical stability is $\omega_{ci}\Delta t < 2$, where ω_{ci} is the ion cyclotron frequency; however, in practice the CFL condition is the more restrictive requirement.

5. RESULTS AND DISCUSSION

To simulate the plasma flow dynamics in the magnetic channel the set of calculations is performed. The main parameters of the calculations are presented below (see Table 1).

Table 1. The main calculation parameters.

Parameters	Run 1	Run 2	Run 3
Plasma energy (J)	1140	2500	2500
Plasma velocity (m/s)	330000	500000	500000
Plasma linear size (X,Y,Z) (m)	0.1×0.04×0.04	0.1×0.04×0.04	0.1×0.04×0.04
Position of plasma centre (m)	(-0.3,0,0)	(-0.3,0,0)	(-0.3,0,0)
Number of coils	2	2	5

Coil radius (m)	0.08	0.08	0.08
Coil current (A)	4.3×10^5	4.3×10^5	1×10^5
Coil position along X (m)	-0.17, -0.25	-0.17, -0.25	-0.19, -0.23, -0.27, -0.31, -0.35
Calculation region (m)	0.7×0.7×0.7	0.7×0.7×0.7	0.7×0.7×0.7

The all plasma particle positions and magnetic field lines for the run 1, which are projected on the ZX plane at initial time, are illustrated in Fig. 2. Also, there are locations of the current coils in this figure.

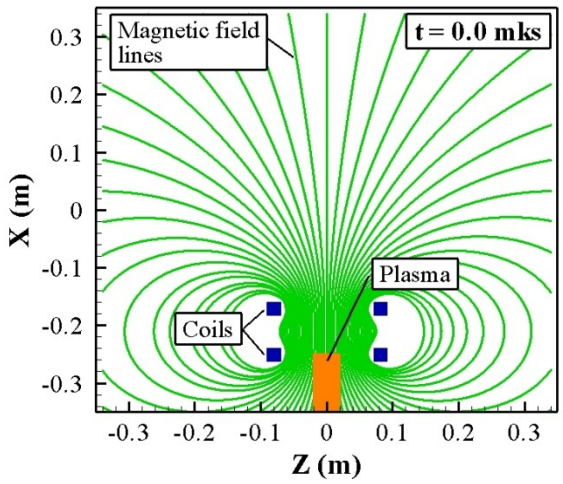


Fig. 2. The magnetic field lines and plasma at initial time (run 1).

Fig. 3 shows the dynamics of all plasma particle locations projected on the same plane. It can be seen that at small velocities the plasma moves along the magnetic field lines and the symmetry of the plasma in the considered plane is conserved.

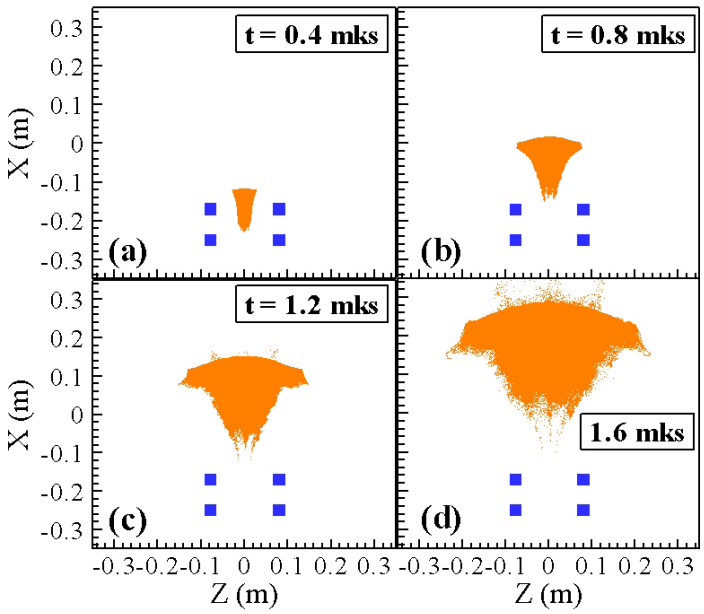


Fig. 3. The dynamics of all plasma particles projected on the ZX plane (run 1): (a) t=0.4*mks*, (b) t=0.8*mks*, (c) t=1.2*mks* and (d) t=1.6*mks*.

A comparison of two runs (run 1 and run 2) is presented in Fig. 4. One can see that in the case (a) there is a minor distortion of the magnetic field lines due to the deficiency of the plasma energy and, also, the noticeable expansion of the plasma. Consequently, there is not enough the plasma kinetic energy for the separation of the plasma from the magnetic field lines in this regime. However, in the case (b) the lines at the outlet of the magnetic channel are curved stronger because of the higher energy.

Fig. 5 illustrates the change of the plasma kinetic energy with time for the run 2. First, on the energy graph one can see oscillations until the time of approximately 0.5 *mks.* This effect deals with the fact that the plasma penetrating into magnetic channel slows down by the coil magnetic field and current. Then, the plasma flow escaping the magnetic channel is accelerated and gives its impulse to the system of the coils.

The dependence of the efficiency factor and time is in Fig. 6. From this graph it is seen that until the time of 0.45 *mks* the efficiency factor of the coils decreases and then starts to increase and is stabilized on the same level from 1.05 *mks* until 1.25 *mks.* As it has been explained in the previous case the plasma loses the energy at the entrance of the magnetic channel and is accelerated by the magnetic field at the channel outlet.

In the run 3, the geometry of the magnetic field had been changed to decrease the energy loss of the plasma at the entrance of the magnetic channel (Fig. 7). Here the initial magnetic field configuration which is generated by five coils and the initial location of the plasma particles are demonstrated. Thereby, the plasma particles start their motion in the uniform magnetic field and move along the magnetic field lines without essential energy losses.

Fig. 8 illustrates the dynamics of all plasma particles and, also, the configuration of the magnetic field lines which are projected on the ZX plane. From this graph it can be seen that the plasma carries along

the magnetic field lines, i. e. it is shown a tendency to the separation of the plasma from the field lines (the plasma does not move along the field lines).

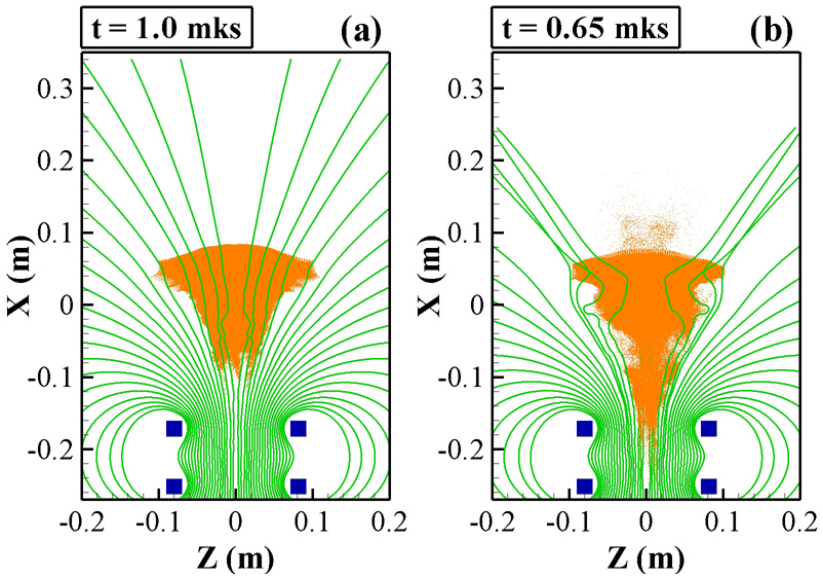


Fig. 4. The plasma particle projections and the magnetic field lines projected on the ZX-plane: (a) run 1 at *t=1mks* and (b) run 2 at *t=0.65mks*.

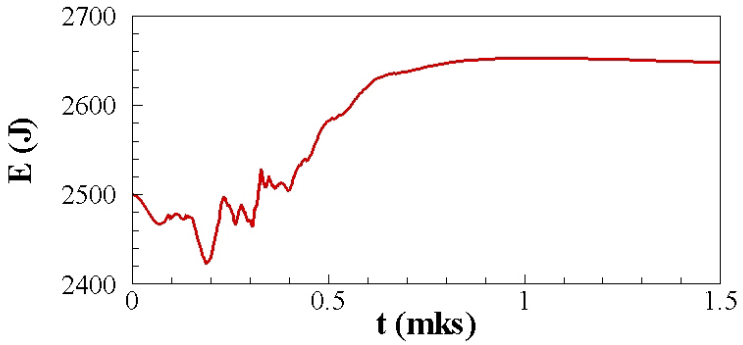


Fig. 5. Plasma energy (run 2).

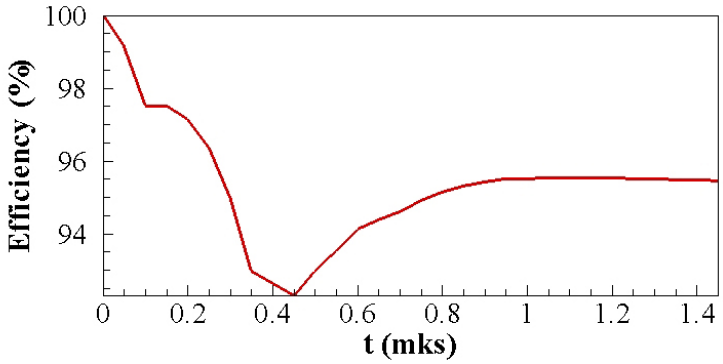


Fig. 6. Efficiency of coil system (run 2).

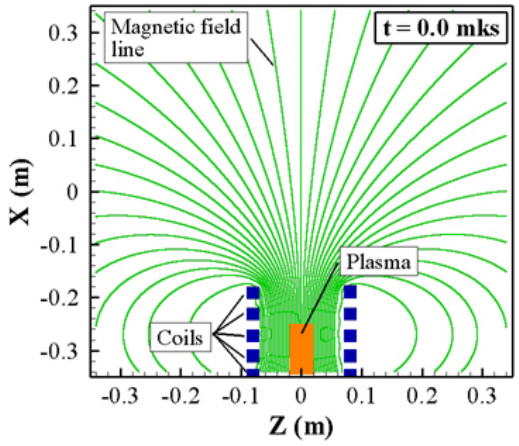


Fig. 7. The magnetic field lines and plasma at initial time (run 3).

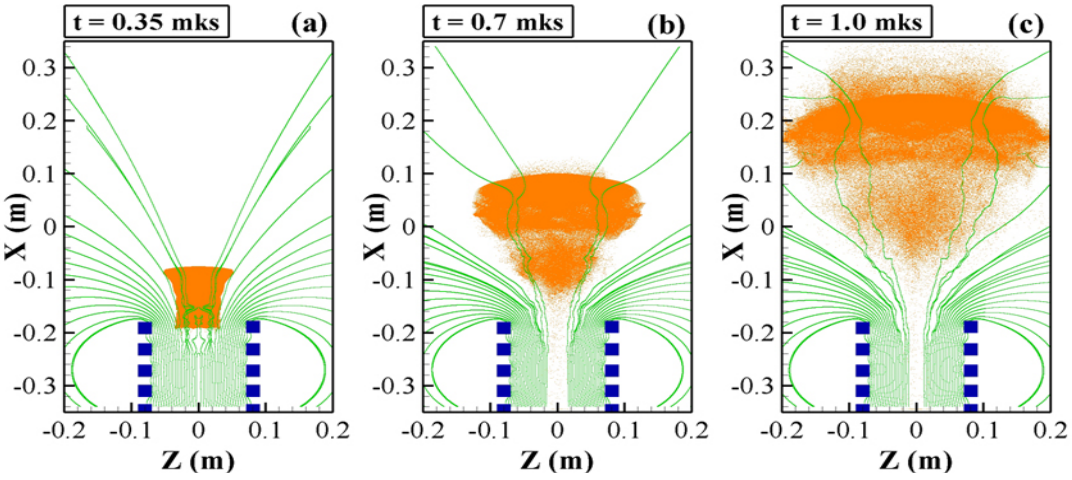


Fig. 8. The all plasma particle projections and the magnetic field lines projected on the ZX-plane (run 3): (a) *t=0.35mks*, (b) *t=0.7mks* and (c) *t=1.0mks*.

6. CONCLUSIONS

The results described in this article show that the magnetic field can accelerate the ions of plasma effectively. The degree of the acceleration can be regulated by the configuration of the magnetic field created by the ring coils and current.

This work can be useful for the investigation of processes in magnetic nozzles.

ACKNOWLEDGEMENTS:

The author of this article thanks Dr. Yu. P. Zakharov and Prof. H. Nakashima for the statement of the problem and, also, Prof. G.I. Dudnikova for useful discussions and advices.

This work has been supported by RFBR grant 09-01-00379.

REFERENCES

1. Gerwin, R.A., Markin, G.J., Sgro, A.G., and Glasser, A.H. (1990) LANL Technical report no. ALTR-89-092.

2. Parker, E.N. (1958) Dynamics of the interplanetary gas and magnetic fields. Astrophys. J. 128, p. 664.

3. Hooper, J.B. (1993) Plasma detachment from a magnetic nozzle. Propul. Power 9, p. 757.

4. Arefiev, A.V., and Breizman, B.N. (2005) Magnetohydrodynamics. Scenario of plasma detachment in a magnetic nozzle. Physics of plasma 12, p. 4.

5. Nagamine, Y., and Nakashima, H. (1999) Analysis of plasma behavior in a magnetic thrust chamber of laser fusion rocket. Fusion technol., 35, pp. 62-70.

6. Vchivkov, K.V., Nakashima, H., Zakharov, Yu.P., Esaki, T., Kawano, T., and Muranaka, T. (2003) Laser –produced plasma experiments and particle in cell simulation to study thrust conversion processes in a laser fusion rocket. Jpn. j. appl. phys., 42, Part 1, pp. 6590-6597.

7. Hockney, R.W., and Eastwood, J.W. (1981) Computer simulation using particles. New York: McGraw-Hill.

8. Harned, S.D. (1982) Quasineutral hybrid simulation of macroscopic plasma phenomena. J. Comp. phys., 47, pp. 452-462.

9. Horowitz, E.J., Shumaker, D.E., and Anderson, D.V. (1989) QN3D: A three-dimensional quasi-neutral hybrid particle-in-cell code with applications to the tilt mode instability in field reversed configurations. J. comp. phys., 84, pp. 279- 310.

10. Tajima, T. (1989) Computational plasma physics: with applications to fusion and astrophysics, Addison - Wesley Publishing Company, Inc.

11. Vshivkov, V.A., Vchivkov, K.V., and Dudnikova, G.I. (2001) Solving algorithms for problem of interaction of laser pulse with plasma. J. comp. tech., 46, No.2, pp. 47-63 [in Russian].

12. Kochin, N.E., Kibel, I.A., and Roze, N.V. (1963) Theoretical hydrodynamics. M: FM, Part 1 [in Russian].